International Compressor Engineering Conference   School of Mechanical Engineering

2018

A Comparison of Thermal Deformation of Scroll Profiles inside Oil-free Scroll Vacuum Pump and Compressor via CAE/CFD Analysis

Sheng-Hung Hsieh
Hanbell Precise Machinery Co., Ltd., Taiwan, Shhsieh@hanbell.com

Jin-Wei Zhang
Hanbell Precise Machinery Co. Ltd., Taiwan, jinwei@hanbell.com

Szu-Pei Chou
Hanbell Precise Machinery Co. Ltd., Taiwan, GasperChou@hanbell.com

Chi-Shun Huang
Hanbell Precise Machinery Co. Ltd., Taiwan, forresthuang@hanbell.com

Follow this and additional works at: https://docs.lib.purdue.edu/icec

A Comparison of Thermal Deformation of Scroll Profiles inside Oil-free Scroll Vacuum Pump and Compressor via CAE/CFD Analysis

Sheng-Hung HSIEH*, Jin-Wei ZHANG, Szu-Pei CHOU, Chi-Shun HUANG

Hanbell Precise Machinery Co. Ltd.
Taoyuan City, Taiwan (R.O.C.)
Phone：+886-4-23501886#23355
Fax：+886-4-23501885
*E-mail：shhsieh@hanbell.com

ABSTRACT

Scroll machine is simply constructed by fixed and orbit scrolls, rotary shaft, and some mechanical components. It can impressively operate at low noise level with high reliability and high efficiency. Scroll machine achieves oil-free application through reasonable clearance control, cooling solution, and the tip seal application, and has been designed and applied as vacuum pump or compressor. In order to compactly design structure and optimize the gaps or clearances of a scroll machine, the issue of heat deformation must be considered. Deformation inside a scroll machine is not easy to be discovered, but is the necessary information for design of scroll profile. In this study, the internal flow fields of oil-free scroll vacuum pump and compressor are obtained by CFD analysis. Based on the results of flow fields, this study shows the basic performance of a scroll machine, including loading on structures, gas torque, volume flow rate, and the pulsation of outlet pressure. The fluid phenomena under sub-atmospheric and positive pressure are quite different. The difference would cause different heat transfer and heat deformation. Therefore, the fluid-thermal-solid coupling analysis is also carried out. The temperature distribution of scroll structures, the thermal deformation, and gap changes are also discussed in this study.

1. INTRODUCTION

The advantages of oil-free scroll machines are compact design, low noise, high reliability, and high efficiency. Oil-free scroll compressor and vacuum pump are now applied in various industries. Technologies for performance analysis of scroll machines are extensively and intensively studied. The analysis tools are well developed and applied in design work. Under the condition of pressure, Kazutaka *et al.* (1988) tried to study deformation of structure of scroll. Rogers *et al.* (1990) practically carried out the CAE/CFD analysis. Yang *et al.* (2010) could precisely predict the abrasion issue of scroll by ANSYS tools. Chang *et al.* (2013) discovered the leakages and pressure distribution inside scroll expander via simulation with 2D dynamic mesh. Wei *et al.* (2015) studied the inlet flow field of a scroll expander and optimized the scroll profiles via simulation with 3D dynamic mesh. Under the condition of vacuum, Cheng *et al.* (1999) showed how to carry out CFD analysis under vacuum. The character of slip flow was discussed. Li *et al.* (2010a; 2010b) did the comparison between experiment and theoretical analysis for an oil-free scroll vacuum pump. Yue *et al.* (2015) analyzed the flow field inside an oil-free scroll vacuum pump via CFD analysis. Hesse *et al.* (2016) well developed software to generate dynamic mesh for scroll machine. They compared results between experiment and simulation, and showed that the pressure curve in scroll vacuum pump is affected by scroll body temperature.

Based on previous studies, the analysis on scroll machine could be carried out efficiently to obtain performance information. In this study, the flow fields in oil-free scroll compressor and vacuum pump are obtained by CFD analysis. With this information, this study also shows force and gas power on orbiting scroll, inlet volumetric flow rate, and outlet pressure curve. The fluid phenomena under pressure and vacuum are quite different. The difference would cause different heat transfer and heat deformation. Therefore, the fluid-thermal-solid coupling analysis is also carried out. The temperature distribution, the thermal deformation, and gap changes are also discussed in this study.

2. THEORETICAL MODEL AND CAE/CFD ANALYSIS

The theoretical models of oil-free scroll compressor and vacuum pump are both established. For an oil-free scroll compressor, the main parts are shown in Figure 1 (a), including a fixed scroll (A), an orbiting scroll (B), a driving plate (C), and a case (D). The compression chamber is constructed by fixed and orbiting scrolls. Orbiting scroll is driven by driving plate. There are inlet, compression and outlet processes in the scroll compressor. The flow path in scroll compressor is shown in Figure 2 (a). Gas flows through inlet part (A) and enters compression chamber (C). After compression, gas would be released through outlet part (B).

For an oil-free scroll vacuum pump, the main parts are shown in Figure 1 (b), including a left fixed scroll (A), a parallel orbiting scroll (B), a right fixed scroll (C), and a driving shaft (D). The chamber is constructed by fixed and orbiting scrolls. Orbiting scroll is driven by driving shaft. There are inlet, transport, compression and outlet processes in scroll vacuum pump. The flow path in scroll vacuum pump is shown in Figure 2 (b). Gas flows through inlet part (A) and enters parallel chambers named (C) and (D). After transport and compression, gas would be released through outlet part (B).

There are two analysis works in this study. The first one is to calculate the flow fields inside oil-free scroll compressor and vacuum pump via ANSYS Fluent. The second one is to analyze thermal deformation by ANSYS structural tool. The flow paths include static and dynamic mesh regions, as shown in Figure 2 (a) and (b). The static mesh regions of both of compressor and vacuum pump are the inlet part (A) and outlet part (B). The dynamic mesh regions are the compression chambers (C) for compressor, and the parallel chambers, (C) and (D), for vacuum pump. The dynamic meshes are controlled by ANSYS Fluent. The element number is about 2,000,000 Cells for compressor, and is about 47,000 Cells for vacuum pump.
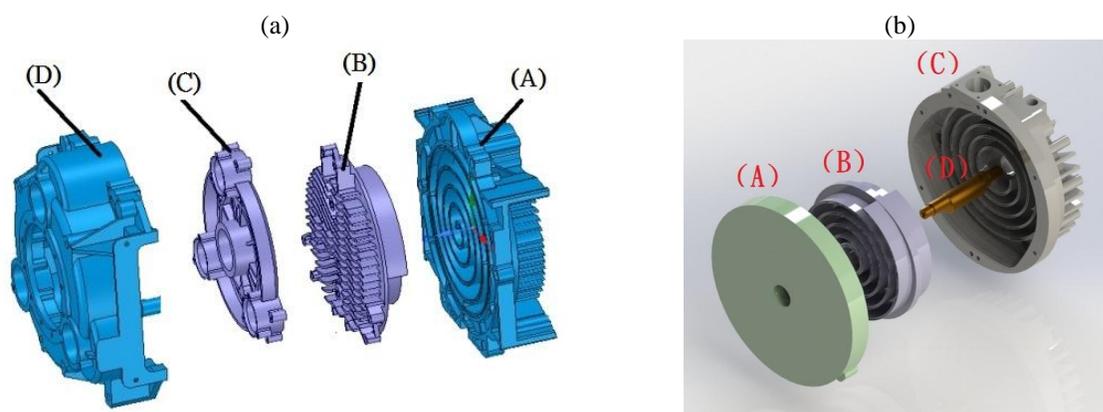
(a)   (b)

Figure 1: The main parts of oil-free scroll compressor (a) and vacuum pump (b)

(a)   (b)
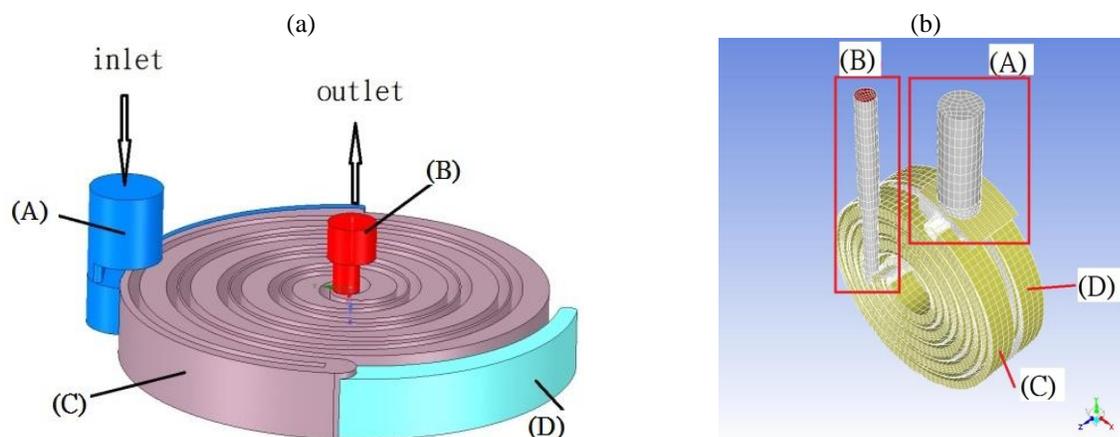

Figure 2: The theoretical models of flow path of oil-free scroll compressor (a) and vacuum pump (b)

The uniform gaps between fixed and orbiting scrolls of compressor and vacuum pump are 0.1mm. The boundary conditions of oil-free scroll compressor are 101,325Pa for inlet pressure, 300K for inlet temperature, 911,925Pa for outlet pressure, and 3,750rpm for rotation speed. When ANSYS Fluent is used in analysis work under vacuum, Knudsen number (Kn) must be considered. Kn shows the continuity of flow under certain conditions of vacuum and geometric scale. Figure 3 (a) shows Kn under different pressure and effective length. The flow field is continuous flow at Kn≦0.01, slip flow at 0.01< Kn≦0.1, and molecular flow at 0.1<Kn. The restriction of theoretical model is that flow field must be continuous flow or slip flow.

For oil-free scroll vacuum pump, there is one interesting phenomenon about power and inlet volumetric flow-rate, as shown in Figure 3 (b). When oil-free scroll vacuum pump operates, inlet pressure continuously decreases. The loading becomes lighter. The inlet volumetric flow-rate becomes higher for the reduced inner leakages. The reduced inner leakage is caused by gas becoming from continuous flow to slip flow or the molecular flow. When the inlet pressure is less than 1,000Pa, the changes of loading is less than 5%. When the inlet pressure is during 100 to 1,000Pa, the minimum inner leakage achieves and the maximum inlet volumetric flow-rate appears. Therefore, with inlet conditions of 800Pa for inlet pressure and 298K for inlet temperature, the calculated information could be meaningful and useful for design works. In this study, the boundary conditions of oil-free scroll vacuum pump are 800Pa for inlet pressure, 298K for inlet temperature, 101,325Pa for outlet pressure, 353K for outlet temperature, and 1,500rpm for rotation speed.
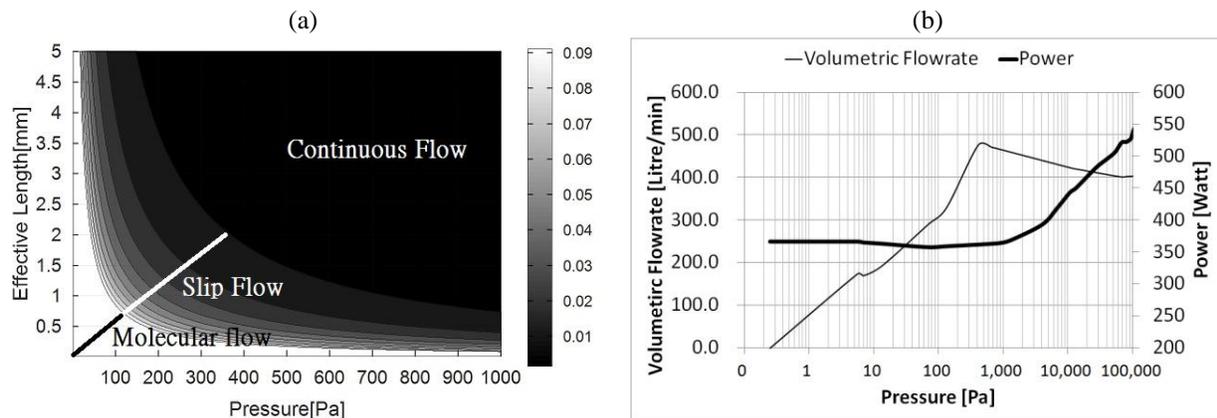

Figure 3: (a) Knudsen number under different pressure and effective length. (b) Performance of an oil-free scroll vacuum pump.

3. RESULT AND DISCUSSION

The theoretical models are calculated to obtain the pressure and flow fields inside oil-free scroll compressor and vacuum pump. In the case of compressor, Figure 4 (a) shows that gas goes into the compression chamber through inlet part. At the start of compression, there is some area at sub-atmosphere. As the orbiting scroll operating, gas is continuously compressed and released through outlet part. In the case of vacuum pump, Figure 4 (b) shows that gas goes into the compression chamber through inlet part. The gas, outside the red circle, experiences the molecular flow and slip flow. As the orbiting scroll operating, gas is continuously transported and compressed. When gas moves into the red circle, the flow becomes to continuous flow. The gas inside the red circle is periodically compressed. This compression process would increase outlet temperature. The leakage flows could be observed on the clearances between orbiting and fixed scrolls of both models of compressor and vacuum pump.
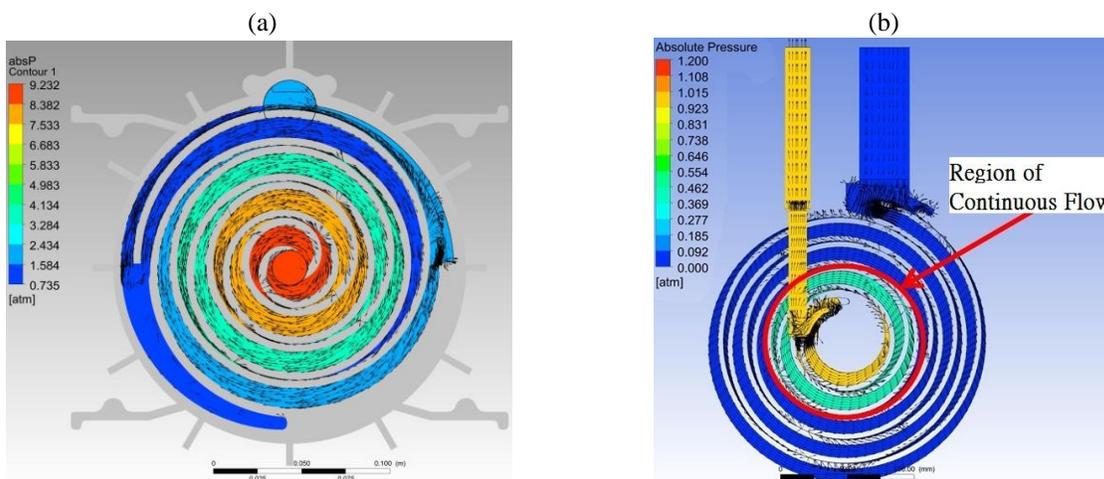
(a)   (b)

Figure 4: Pressure distributions and flow fields in oil-free scroll compressor (a) and vacuum pump (b)

The inlet volumetric flow-rate curves are shown in Figure 5. In the case of compressor, Figure 5 (a) shows the average flow-rate is about 406L/min. There is one major pulse during a rotation cycle. The value on pulse crest is about two times of average value. The value on pulse through is close to 0L/min. It is evident that the surge of inlet flow of compressor is large. In the case of vacuum pump, Figure 5 (b) shows the average flow-rate is about 472L/min. There are two pulses appear in the ranges from (A) to (B) and from (C) to (D) during a cycle. The trends of arising of these two pulses, (A) and (C), are quite the same. The trends of dropping of these two pulses, (B) and (D), are different. This is affected by the geometric difference between inner and outer chambers, which are separated by orbiting scroll.
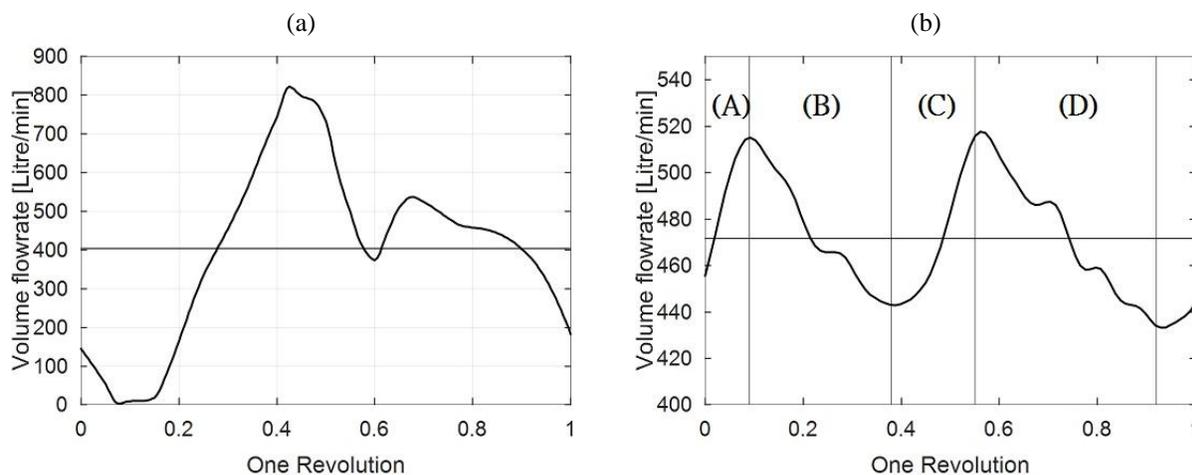
(a)   (b)

Figure 5: Inlet volumetric flow-rates of oil-free scroll compressor (a) and vacuum pump (b)

Figure 6 shows the outlet gauge pressure curves during an operation cycle. In the case of compressor, Figure 6 (a) shows that the outlet pressure curve is smooth with a little drop. In the case of vacuum pump, Figure 6 (b) shows that there is an observable pulse during a quarter of one cycle. When the outlet port is just opened, the pressure in the compression chamber is less than the backing pressure. Therefore, the gas would rush back from outlet part to the compression chamber. The outlet pressure goes through ups and downs, and becomes constant as the gas in compression chamber and re-entered gas being mixed well and pushed out together.
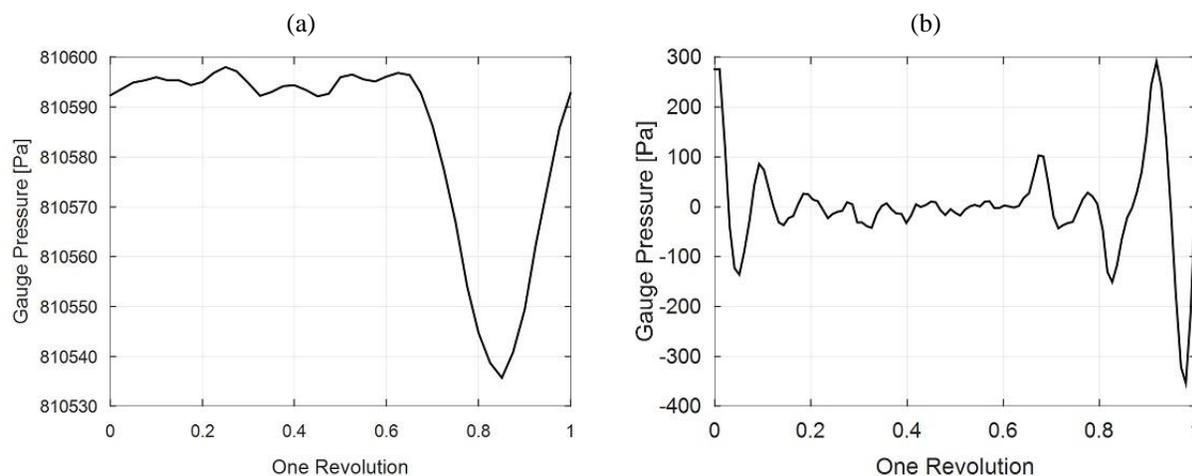
(a)   (b)

Figure 6: Outlet pressures of oil-free scroll compressor (a) and vacuum pump (b)

The pressure information is used in calculating the forces on orbiting scroll. In the case of compressor, Figure 7 (a) shows the radial force on orbiting scroll is about 2131N. The forces on x and y directions change when orbiting scroll operates. In the case of vacuum pump, Figure 7 (b) shows the radial force on orbiting scroll is about 515N. The forces on x and y directions also change when orbiting scroll operates. Both in compressor and vacuum pump, the variants of radial force are small. The direction of force whirls when orbiting scroll operates.
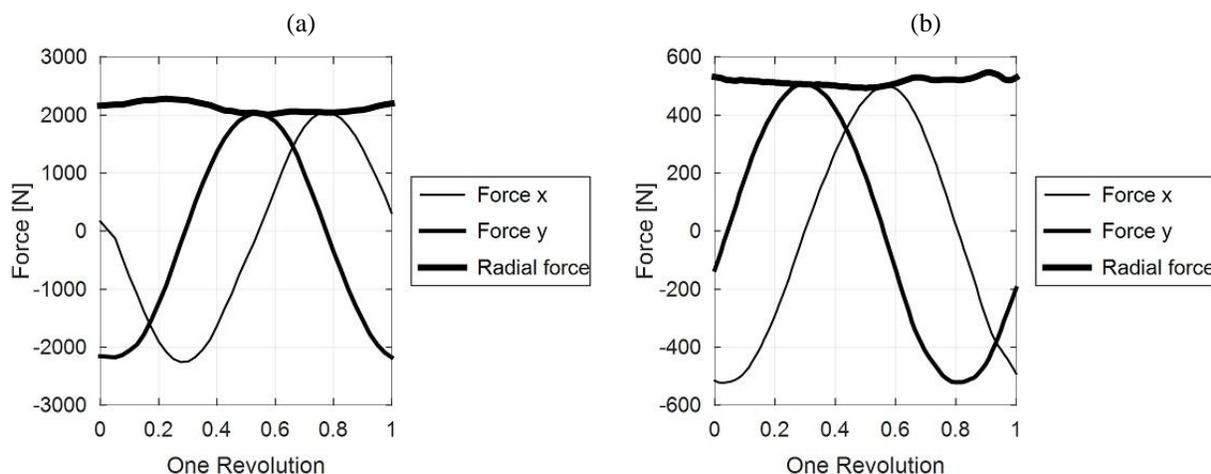
(a)   (b)

Figure 7: The forces on orbiting scroll of oil-free scroll compressor (a) and vacuum pump (b)

The gas power curves are shown in Figure 8. In the case of compressor, Figure 8 (a) shows the average gas power on orbiting scroll is about 3141.63W. The gas power curve is smooth with a little drop. In the case of vacuum pump, Figure 8 (b) shows the average gas power on orbiting scroll is about 114W. The positive value of gas power means loading of motor. In certain range during a cycle, the negative gas power appears and loading on motor would be lighter. The positive and negative gas powers appear during a rotation cycle. Stability of orbiting scroll of vacuum pump would be influenced.
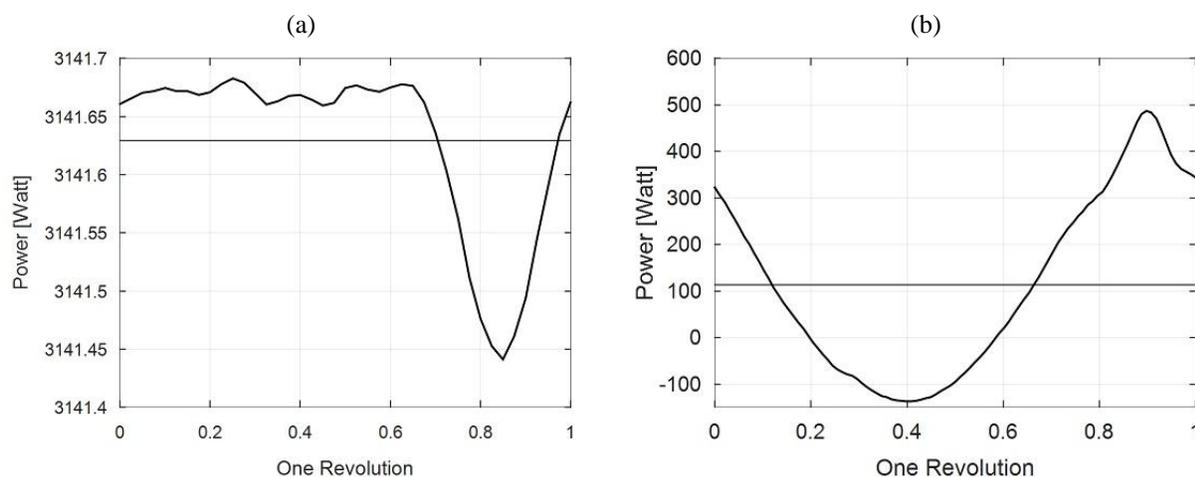
Figure 8: Gas powers on orbiting scroll of oil-free scroll compressor (a) and vacuum pump (b)

Figure 9 (a) shows the temperature distribution inside the oil-free scroll compressor. Temperature of scroll is raised by the compression energy. The maximum value is about 520K. For the cooling effect on case and scrolls, the temperature decreases outward from the center. Figure 9 (b) shows the temperature distribution inside the oil-free scroll vacuum pump. Part of scroll experiences lower pressure space, where heat transfer is less. The other part experiences higher pressure space, where heat transfer is more. High temperature appears near the center of orbiting scroll. The highest temperature is about 364K. For the cooling effect on fixed scrolls, the temperature decreases outward from the center.
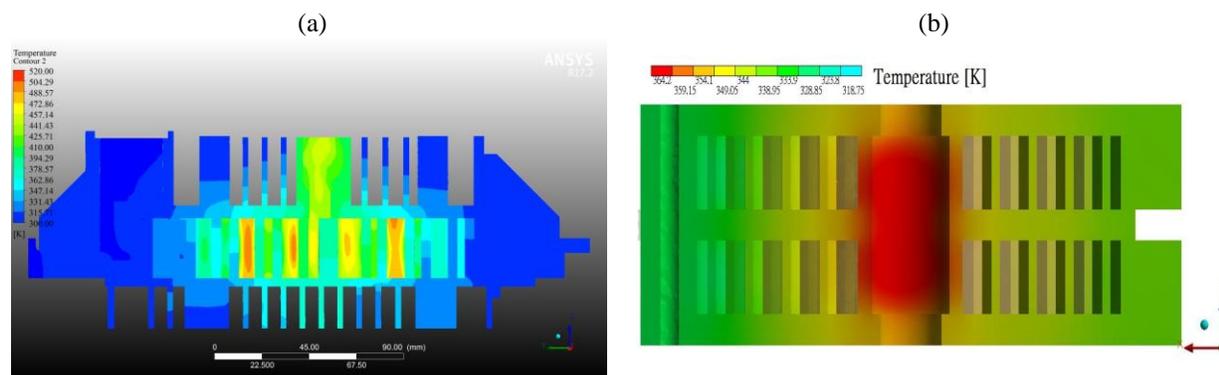

Figure 9: Temperature distributions on oil-free scroll compressor (a) and vacuum pump (b)

The uniform axial clearances of compressor and vacuum pump are 0.1mm. Based on the temperature information, the thermal deformation is calculated. Figure 10 shows the axial deformation and the remained axial clearances of scroll profiles of oil-free scroll compressor and vacuum pump. Figure 10 (a) and (d) show that the axial deformation data locate form center toward outside of scroll profiles.

In the case of oil-free scroll compressor, Figure 10 (b) shows the axial deformation on orbiting scroll bottom is from 0.05mm to 0mm. The axial deformation on fixed scroll tip is from 0.01mm to 0.07mm. The remained axial clearance is from 0.05mm to 0.15mm. Figure 10 (c) shows the axial deformation on orbiting scroll tip is from 0.05mm to 0.08mm. The axial deformation on fixed scroll bottom is from 0.12mm to 0.02mm. The remained axial clearance is from 0.15mm to 0.05mm.

In the case of oil-free scroll vacuum pump, Figure 10 (e) shows the axial deformation on orbiting scroll bottom is near 0.01mm. The axial deformation on fixed scroll tip is also near 0.01mm. The remained axial clearance is closed to 0.1mm. Figure 10 (f) shows the axial deformation on orbiting scroll tip is from 0.06mm to 0.02mm. The axial deformation on fixed scroll bottom is also from 0.06mm to 0.02mm. The remained axial clearance is between 0.08mm and 0.12mm. The raised temperature in oil-free scroll vacuum pump is less than the one in compressor. The

deformation in vacuum pump is much more uniform than the one in compressor. The remained axial clearance in the oil-free scroll vacuum pump could be closed to the designed value.
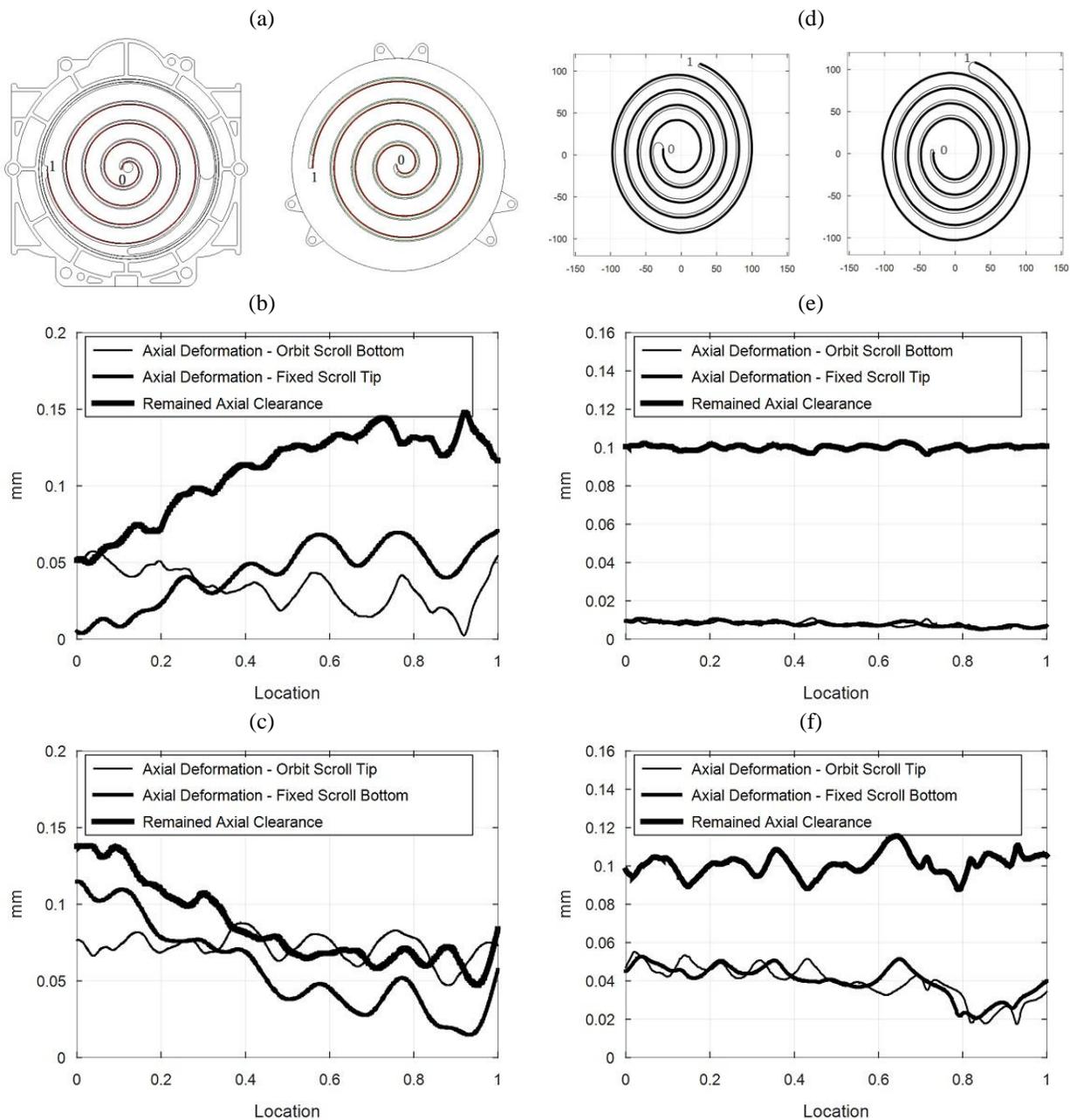

Figure 10: The data of axial thermal deformation and remained clearance are located form center toward outside of oil-free scroll compressor (a) and vacuum pump (d). The graphs of (b) and (c) are axial clearances in compressor, and (e) and (f) are axial clearances in vacuum pump.

4. CONCLUSIONS

The outlet pressure, inlet volumetric flow-rates, force and gas powers on orbiting scroll of oil-free scroll compressor and vacuum pump are calculating by dynamic mesh and CFD tools. The fluid phenomena in scroll compressor and vacuum pump are quite different. This would cause different heat transfer and thermal deformation. Temperature inside the oil-free scroll compressor is increased by compression energy. The maximum value is about 520K. The temperature decreases outward from the center. For vacuum pump, part of scroll experiences low pressure space, where heat transfer is less. Part of scroll experiences higher pressure space, where heat transfer is more. The highest temperature is about 364K. The temperature decreases outward from the center. The raised temperature of oil-free scroll vacuum pump is less than compressor. The deformation in vacuum pump is much more uniform than the one in compressor. The remained axial clearance in the oil-free scroll vacuum pump could be closed to the designed value.

REFERENCES

Chang, C. W., Chang, J. C., Hung, T. C. & Tseng, Y. S. (2013). CFD simulation and experiment of scroll expander for organic Rankine systems. *Advanced Materials Research*, Vols. 614-615, pp 515-519.

Cheng, H. P., Jou, R. Y., Chen, F. Z., Chang, Y. W., Matsumi, I., & Takashi, H. (1999). Flow investigation of Siegbahn vacuum pump by CFD methodology. *Vacuum*, Vol. 53, pp. 227-231.

Hesse, J., & Andres, R. (2016). CFD Simulation of a Dry Scroll Vacuum Pump Including Leakage Flows. *International Compressor Engineering Conference*, Purdue.

Kazutaka, S., Masao, S., Rumi, M., & Kenji, T. (1988). Deformation Analysis of Scroll Members in Hermetic Scroll Compressors for Air Conditioners. *International Compressor Engineering Conference*, pp. 674.

Li, Z., Li, L. S., Zhao, Y. Y., Bu, G. X., & Shu, P. C. (2010). Theoretical and experimental study of dry scroll vacuum pump. *Proceedings of the Vacuum*, Vol. 84, pp.415-421.

Li, Z., Li, L. S., Zhao, Y. Y., Bu, G. X., Shu, P. C., & Lui, J. P. (2010). Test and analyses on the working process of dry scroll vacuum pump. *Proceedings of the Vacuum*, Col. 85, pp.95-100.

Rogers, R. J., & Wagner, R. C. (1990). Scroll Compressor Flow Modeling: Experimental and Computational Investigation. *International Compressor Engineering Conference*, pp. 707.

Wei, M., Song, P., Zhao, B., Shi, L., Wang, Z., & Ma, C. (2015). Unsteady flow in the suction process of a scroll expander for an ORC waste heat recovery systems. *Applied Thermal Engineering*, Vol. 78, pp. 460-470.

Yue, X. J., Lu, Y. J., Zhang, Y. L., Ba, D. C., & Wang, G. Y. (2015). Computational fluid dynamics simulation study of gas flow in dry scroll vacuum pump. *Proceedings of the Vacuum*, Vol. 116, pp.144-152.

Yang, Y. B., Tang, Y. J., & Chang, Y. C. (2010). Static and Dynamic Analysis on R410A Scroll Compressor Components. *International Compressor Engineering Conference*, pp. 1958.